Available online at www.sciencedirect.com
ScienceDirect
Acta Materialia 58 (2010) 1530–1535
Acta MATERIALIA
www.elsevier.com/locate/actamat

Full elastic tensor of a crystal of the superhard compound ReB_2

J.B. Levine [a], J.B. Betts [b], J.D. Garrett [c], S.Q. Guo [d], J.T. Eng [a], A. Migliori [b,*], R.B. Kaner [a,e,*]

[a] Department of Chemistry and Biochemistry and California NanoSystems Institute, University of California, Los Angeles, CA 90095-1569, USA
[b] National High Magnetic Field Laboratory, Los Alamos National Laboratory, Los Alamos, NM 87545, USA
[c] Brockhouse Institute for Materials Research, McMaster University, Hamilton, Ontario, Canada L8S 4M1
[d] Composites Group, National Institute for Materials Science, Tsukuba 3050047, Japan
[e] Department of Materials Science and Engineering, University of California, Los Angeles, CA 90095-1595, USA

Received 17 July 2009; received in revised form 29 October 2009; accepted 30 October 2009
Available online 7 December 2009

Abstract

The search for superhard materials, driven by their widespread use in industrial applications, highlights one of the most difficult problems in the field of materials science: the accurate characterization of a material's intrinsic physical properties. This paper reports on the full elastic tensor of two polycrystalline isotropic specimens and one specimen of ReB_2 consisting of highly oriented grains. The high-monocrystal bulk modulus value extracted from the grain-oriented specimen, measured by resonant ultrasound spectroscopy, validates the ultra-incompressibility of ReB_2. An observed hardness of 40 GPa and a Debye temperature of 731 K were calculated for the ReB_2 crystal, confirming its superhard and super-stiff properties. All the measured moduli of the ReB_2 grain-oriented crystal exceed the comparable ones for the polycrystal by amounts that cannot be explained by averaging over direction, which may reveal why recent measurements reported on ReB_2 containing excess boron yield values that are not as hard or incompressible as the crystal.

Keywords: Borides; Elastic moduli; Hardness; Resonant ultrasound spectroscopy; X-ray diffraction

1. Introduction

Some dense transition metal borides possess extreme mechanical properties, including high hardness and low compressibility [1–8]. Because of the economic and technological importance of such properties, much theoretical work has focused on understanding the extreme hardness, and on the tools needed to predict the composition of other superhard compounds [9–18]. There has been considerable controversy surrounding measurements and models of ReB_2, where some experimental and first-principles approaches [16,18,19] have failed to agree with previous studies by Chung et al. [2,3] and Levine et al. [8]. For example, Qin et al. [20] prepared densified composites of ReB_2 and determined the hardness and the elastic moduli via ultrasonic measurements using a pulse-echo method [20]. They found ReB_2 to be neither superhard nor ultra-incompressible, and determined surprisingly low values for both Young's modulus (382 GPa) and shear modulus (173 GPa). This paper reports on the full elastic tensor for a ReB_2 crystal consisting of grains oriented with their hexagonal axes parallel, hereafter called the crystal, and two types of polycrystalline ReB_2. The crystal is found to be superhard and ultra-incompressible ($B = 383$ GPa), but substantial variation is found in the polycrystalline specimens, and a likely origin of the discrepancies among the studies of this material is suggested.

2. Materials and methods

Three specimens of ReB_2 with intentionally contrasting morphologies were synthesized: (1) a densified compact of

* Corresponding authors. Addresses: National High Magnetic Field Laboratory, Los Alamos National Laboratory, Los Alamos, NM 87545, USA (A. Migliori), Department of Chemistry and Biochemistry and California NanoSystems Institute, University of California, Los Angeles, CA 90095-1569, USA (R.B. Kaner).
E-mail addresses: migliori@cybermesa.com (A. Migliori), kaner@chem.ucla.edu (R.B. Kaner).

1359-6454/$36.00 © 2009 Acta Materialia Inc. Published by Elsevier Ltd. All rights reserved.
doi:10.1016/j.actamat.2009.10.060

ReB_2 prepared by spark plasma sintering (SPS); (2) a high-purity crystal with grains oriented with respect to the *c*-axis, prepared at ambient pressure using a tri-arc crystal-growing furnace; and (3) an arc-melted ingot of ReB_2. The last specimen was included because its polycrystalline microstructure can be compared to the densified compact, while the method of synthesis and purity is similar to the tri-arc crystal.

For the densified compact, ReB_2 powder was initially synthesized via a stoichiometric reaction between rhenium metal (Rhenium Alloys, Inc., −325 mesh, 99.99%) and amorphous boron (Cerac, Inc., size $\leqslant$ 1 μm, 99.9%). The reaction occurred in vacuum in a resistively heated furnace at 750 °C for 72 h with a heating and cooling rate of 100 °C h^{-1}. After confirming the purity of the sample by powder X-ray diffraction, 10% excess boron was added to ensure that the sample remained single phase. Without excess boron, Re_7B_3 forms during the sintering process. The powder was loaded into a graphite die lined with graphite foil, with inner diameter 10 mm. SPS at 1850 °C and 50 MPa (die compression) for 180 s in vacuum ($\sim 6 \times 10^{-2}$ Pa), with a heating rate of ~300 °C min^{-1} produced an ReB_2 pellet ~10 mm in diameter and 2 mm thick with a density of 10.89 g cm^{-3} (85.9% of the theoretical density of 12.68 g cm^{-3} for ReB_2) [21].

The ReB_2 crystalline boule was produced in a modified tri-arc crystal-growing apparatus. A crystal was pulled at 25 mm h^{-1} with hearth (120 rpm) and Mo seed rod (27 rpm) counter-rotating. The initial material was solidified from a previously arc-melted ingot with composition $ReB_{2.05}$. The extra 0.05 mol of boron compensates for B evaporation. A final density of 12.51 g cm^{-3} (98.7% of theoretical density) was obtained for the sample using Archimedes' principle and a water immersion technique. The arc-melted ingot was prepared following Ref. [2] with a final density of 11.12 g cm^{-3} (87.7% of theoretical density).

Powder X-ray diffraction patterns were collected on an XPert Pro powder diffractometer (PANalytical) with Cu K_α radiation ($\lambda = 1.5418$ Å). For the tri-arc specimen, additional crystallographic data were collected on a D8 Discover diffractometer with a Hi-Star area detector (Bruker) with the X-ray beam centered on the (0 0 2) face. A Nano Indenter XP (MTS Systems Corp.) was used to measure hardness on samples encased in a slow-curing epoxy resin and polished using silicon carbide abrasive paper and diamond films (particle sizes 30, 15, 6, 3 and 1 μm) to obtain a mirror finish. Hardness values were calculated in situ by the method of Oliver and Pharr [22].

The elastic moduli C_{ij} were measured using resonant ultrasound spectroscopy (RUS) at ambient temperature (295 K). Specimens were positioned in weak contact with two broadband piezoelectric transducers. Frequency sweeps were made, and the resulting macroscopic mechanical resonances in the specimen were detected. The elastic constants were then calculated from the frequencies, sample mass and dimensions, and the known crystal symmetry (the so-called inverse problem). A more detailed description of the process can be found elsewhere [23–26].

3. Results and discussion

The powder X-ray diffraction pattern for a crushed portion of the tri-arc boule is shown in Fig. 1. All specimens were indexed according to JCPDS file 00–011-0581, confirming the synthesis of ReB_2 for each. Although the powder pattern for the densified compact (not shown) indicates a single-phase compound, it is important to emphasize that the sample contains amorphous boron distributed between the ReB_2 grains (i.e., $ReB_2 + 0.2B$) confirmed by energy dispersive X-ray spectroscopy in a scanning electron microscope, and corroborated by the low sample density. This excess boron has a pronounced effect on the mechanical properties, as discussed below. A powder diffraction

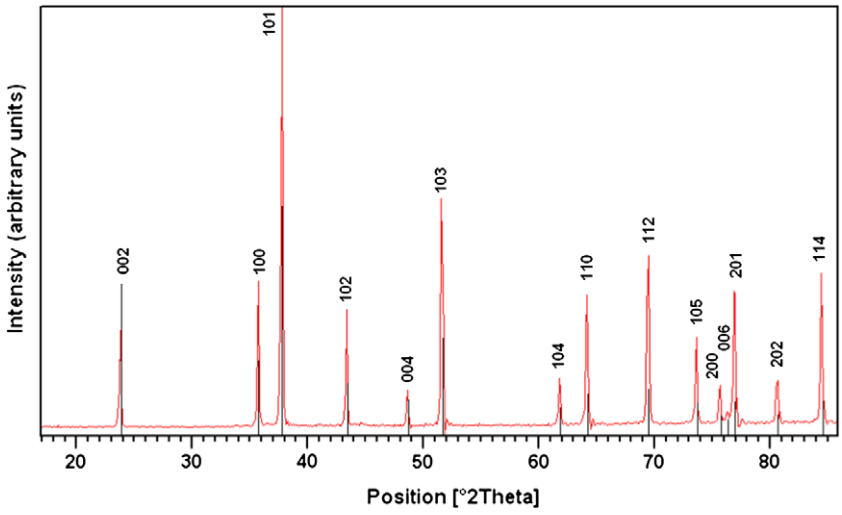

Fig. 1. Powder X-ray diffraction pattern for pulverized ReB_2 powder prepared from the tri-arc crystal. The pattern is indexed according to the JCPDS # 00–011-0581 for ReB_2 which is shown as a stick pattern.

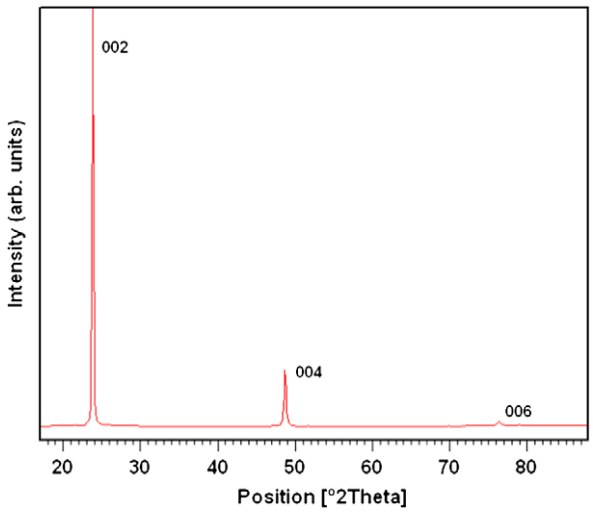

Fig. 2. Powder X-ray diffraction pattern for the as-grown tri-arc crystal oriented with respect to the *c*-axis. Only three diffraction peaks are present corresponding to {0 0 ℓ}.

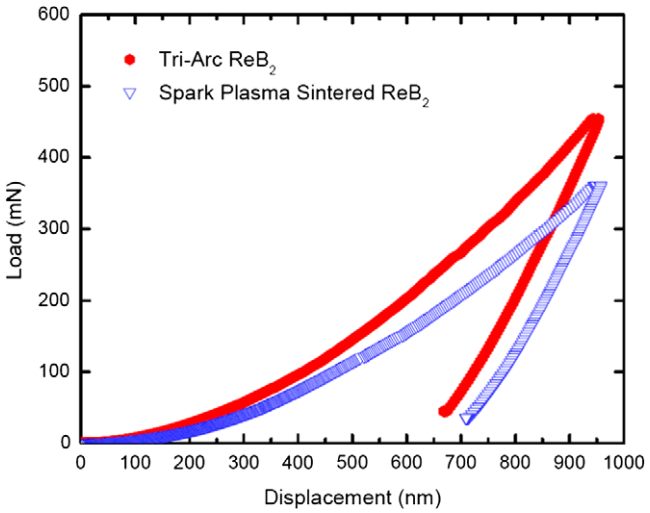

Fig. 3. Load–displacement curves for the ReB_2 tri-arc crystal and SPS compact obtained from nanoindentation experiments.

pattern for the tri-arc crystal cut perpendicular to the growth direction is shown in Fig. 2, with only three peaks present, corresponding to the (0 0 2), (0 0 4) and (0 0 6) planes. Additional diffraction measurements on the tri-arc crystal were collected using the Bruker D8 discover diffractometer centered on the (0 0 2) face. The radiation was monochromatized and parallelized using Göbel mirror optics ($K_{\alpha 1} = 1.54050$ Å) and collimated to produce a 1000-μm beam diameter. Three data frames were collected using 0.5° ω scans at 2θ values of 25.0°, 50.0° and 70.0°. The resulting data indicate that the specimen is actually a highly oriented polycrystalline sample with an average crystallite size of 250(1) Å. The ideal ratio between the 0 0 2 peak and the peak with the highest intensity, 101, is 0.64, as determined by La Placa and Post [21], but in the present sample the actual peak ratio is 33 (not shown in Fig. 2). The highly oriented nature of the crystal along {0 0 ℓ} suggests that the polycrystallinity is caused by twinning which occurred during the growth process, probably from 60° rotations in the *ab* plane, similar to what was observed for flux-grown ReB_2 crystals [8]. ReB_2 synthesized in an optical floating zone furnace was also shown to grow in the ⟨0 0 ℓ⟩ direction, in agreement with our observations [27].

For hardness testing, A Berkovich diamond nanoindenter was used to penetrate from 200–800 nm beneath the specimen surface to eliminate any surface effects. Hardness values were determined as follows: for the SPS compact 27.0 ± 4.7 GPa, and for the crystal 39.5 ± 2.5 GPa (Fig. 3). As shown in Fig. 3, for a given applied load, the diamond indenter penetrates deeper into the SPS sample than the crystal, indicating lower resistance to plastic deformation and lower hardness. Qin et al. recently claimed that ReB_2 is not superhard, because they obtained microhardness values of ~18 GPa for a densified compact of ReB_2. However, their synthetic procedure required 25% excess boron to produce a single-phase compound, as determined by powder X-ray diffraction (Fig. 2 in Ref. [20]). A weakness of purity measurements using powder X-ray diffraction is that (aperiodic) amorphous boron is not detectable. The consequences of adding excess boron is evident. For example, despite the lower density of the present specimen (10.89 vs. 12.0 g cm^{-3} reported for Qin et al.), a hardness that is 56% higher was observed, most likely because the synthetic method presented here only required an additional 10% boron. Note also that the hardness of the present SPS sample is within the range of values reported previously for SPS compacts of ReB_2 [28].

The measured hardness of the tri-arc crystal, 39.5 ± 2.5 GPa, classifies this material as superhard and is the highest reported value for ReB_2 obtained so for via nanoindentation [2,3,8]. This is attributed to the high density (12.51 g cm^{-3}) and purity. The hardness of flux-grown ReB_2 [8] was lower probably because of aluminum inclusions and a boron-deficient network, similar to other diboride crystals grown using the flux method [29]. The tri-arc crystal growth method, which is crucible-free, minimizes impurities, because no container contacts the material. Although different synthetic methods are expected to yield different properties, the range of values for hardness (from 18 to 40 GPa for bulk samples) and elastic moduli presented below is surprising.

The elastic modulus tensor of hexagonal-symmetry monocrystalline ReB_2 (point group: $P6_3/mmc$) requires five independent entries. One choice of which values to present is the set of C_{33}, C_{23}, C_{12}, C_{44} and C_{66}. In systems with hexagonal symmetry, the requirements for rotation of the fourth-rank-tensor elastic moduli about the axis perpendicular to the hexagonal plane and the requirement that the physical properties be sixfold rotationally invariant require that the elastic tensor components exhibit cylindrically isotropic properties. Of particular interest here is that the compressional and shear stiffnesses in the plane perpendicular to

the hexagonal axis are, unlike any other elastic symmetry in a principle crystallographic direction, isotropic. Thus, the shear stiffness $C_{66} = (C_{11} - C_{12})/2$.

For the purposes of measurement validity, this means that it is not necessary to orient the hexagonal plane with specimen faces to obtain accurate monocrystalline moduli, nor are the measured moduli affected by grains of arbitrary orientation in the hexagonal plane as long as their hexagonal axes are aligned. Thus, in ReB_2, any ultrasonic measurement of either a single crystal or a polycrystal with multiple grains with aligned hexagonal axes produces identical and correct monocrystal values. Thus, the present results, though for polycrystalline samples, are the correct monocrystal values because of hexagonal symmetry and grain alignment. Furthermore, errors in the off-diagonal moduli are less pronounced, because these moduli always appear in combination with diagonal moduli when determining an elastic wave speed.

The elastic moduli measured are shown in Table 1 for the three different specimens of ReB_2 and are compared with theoretical calculations using the generalized gradient approximation (GGA) [9]. Because the SPS compact and arc-melted ingot are randomly oriented polycrystalline materials, an isotropic model was used, requiring only two independent moduli, because $C_{11} = C_{33}$, $C_{44} = C_{66}$ and $C_{12} = C_{13}$ and $C_{66} = (C_{11} - C_{12})/2$. The calculated GGA values reported by Hao et al. [9] agree moderately well with the experimental values for the tri-arc specimen, except for an underestimation of C_{12} and C_{13}. As mentioned above, the big errors in these moduli produce small errors in any physically measured wave speed. The SPS compact, however, has substantially lower values, as expected, because of the lower density and excess boron.

For estimations of polycrystalline moduli from monocrystalline elastic moduli, the Voigt model expresses the stress in a single crystal in terms of the given strain, whereas the Reuss model expresses the strain in terms of the given stress [30,31]. It is worth noting that, for hydrostatic stress conditions, the bulk modulus is an invariant between mono- and polycrystals. For the hexagonal-symmetry element Be, this was, in fact, observed to be accurate to within a few tenths of a per cent [32]. Neither model is particularly useful except to set possible boundary conditions. The procedure that is most accurate requires averaging of the wave equations over thousands of directions in space. However, the authors do not have a code for this process in hexagonal symmetry and simply provide the Reuss–Voight average suggested by Hill [33]. For a hexagonal crystal, the two equations for the Voigt moduli are:

$$G_V = \frac{1}{15}(2C_{11} + C_{33} - C_{12} - 2C_{13}) + \frac{1}{5}(2C_{44} + C_{66}) \quad (1)$$

$$B_V = \frac{1}{9}(2C_{11} + C_{33}) + \frac{2}{9}(C_{12} + C_{13}) \quad (2)$$

where C_{ij} are the elastic stiffness tensors [31]. The formulae for the Reuss moduli are given by:

$$G_R = \frac{15}{4(2S_{11} + S_{33}) - 4(S_{12} + 2S_{13}) + 3(2S_{44} + S_{66})} \quad (3)$$

$$B_R = \frac{1}{(2S_{11} + S_{33}) + 2(S_{12} + 2S_{13})} \quad (4)$$

where S_{ij} are the elastic compliance tensors (obtained by inverting the C_{ij} matrix) [30]. Hill showed that, empirically, the actual bulk and shear moduli fall between the Voigt and Reuss models [33], thus:

$$B_H = \frac{1}{2}(B_R + B_V) \quad (5)$$

$$G_H = \frac{1}{2}(G_R + G_V) \quad (6)$$

Additionally, the Young's modulus and the Poisson's ratio can be expressed by the following relationships [33]:

$$\frac{1}{E} = \frac{1}{3G} + \frac{1}{9B} \quad (7)$$

$$\nu = \frac{1}{2}\left[1 - \frac{3G}{3K + G}\right] \quad (8)$$

Table 2 shows the elastic moduli for the tri-arc crystal, SPS compact, arc-melted ReB_2 and theoretical models. In all cases, it was assumed that the compact and polycrystalline ingots were isotropic, and the tri-arc crystal estimates are the Voigt–Reuss–Hill approximations for a hexagonal crystal. The tri-arc crystal has the highest elastic moduli of the three specimens, with the theory in very good agreement. It is noted that the approximate error bars for the measurements are as follows: C_{33} 0.8%; C_{23} 5%; C_{12} 2.5%; C_{44} and C_{66} 0.1%. The average shear modulus of 273 GPa exceeds the shear modulus of c-BC_2N (238 GPa, as determined by spectroscopic methods), the second hardest reported material [34,35]. Note that even without

Table 1
Elastic constants for three forms of ReB_2.

	C_{11}	C_{33}	C_{44}	C_{66}	C_{12}	C_{13}
Tri-arc[a]	674	1023	269	241	192	185
SPS compact[a]	474		183		108	
Arc-melted[a]	650		266		119	
GGA approx.[b]	668	1063	273	266	137	147

[a] A hexagonal model is used for the hexagonally oriented tri-arc sample to determine all the elastic constants, whereas the SPS and arc-melted specimens are randomly oriented polycrystalline materials and therefore require an isotropic model.

[b] The theoretical values determined using a GGA are from Ref. [9].

Table 2
Elastic moduli, Poisson's ratio and densities for the three forms of ReB_2 obtained from the experimentally derived elastic constants along with theoretical calculations.

	E	B	G	ν	ρ (g cm^{-3})
Tri-arc	661	383	273	0.21	12.51
SPS compact	434	230	183	0.19	10.89
Arc-melted	614	296	267	0.15	11.12
GGA approx.	683	355	289	0.18	12.96

averaging, the minimum shear modulus of the crystal also exceeds the reported value for c-BC_2N. The bulk modulus of 383 GPa falls within the upper limits of the bulk modulus determined by in situ high-pressure diffraction experiments (360–390 GPa) [2]. The elastic moduli of the powder compact are significantly lower than those of the tri-arc specimen, probably because of the low density and excess boron, suggesting that the ultrasound values for moduli presented by Qin et al. were not intrinsic properties of ReB_2.

Koehler et al. [36] recently determined the elastic moduli of polycrystalline arc-melted ReB_2 as a function of temperature from 5 to 325 K by RUS and Voigt–Reuss–Hill averaging. The values obtained at 300 K are in excellent agreement with the present values; the bulk, shear and Young's moduli reported in Table 1 for arc-melted ReB_2 all fall within 10% of the values reported in Ref. [36]. The arc-melted sample, being composed of large randomly oriented crystallites of ReB_2 (100–300 μm in length) and containing relatively little amorphous boron, has both a Young's and a shear modulus in good agreement with the tri-arc crystal, differing only by 8% and 2%, respectively. The arc-melted ingot values for E and G are closer to the tri-arc sample than for the SPS compact, despite the ingot having a nearly equivalent density to the compact: 11.12 vs. 10.89 g cm^{-3}, respectively. This suggests that although density plays an important role in the mechanical properties, excess boron (as little as 10%) strongly degrades hardness and bulk modulus.

ReB_2 is significantly elastically anisotropic. C_{33}, with a value of 1023 GPa, is very close to C_{11} for diamond, 1078 GPa (determined using RUS [37]), explaining why ReB_2 is as incompressible as diamond along the c-axis [2]. The elastic anisotropy can be more accurately analyzed by examining the ratio of the principle Young's moduli E_{ii}, calculated by taking the inverse of the corresponding elastic compliances:

$$E_{ii} = \frac{1}{S_{ii}} \tag{9}$$

The values are presented in Table 3. The values for the tri-arc crystal are $E_{11} = 602$ GPa and $E_{33} = 944$ GPa, giving a Young's modulus ratio $E_{33}/E_{11} = 1.57$, indicating substantial elastic anisotropy. These values agree within expected experimental errors with the elastic moduli and the indentation moduli observed for the (0 0 2) and (h k 0) planes of flux-grown ReB_2 [8].

Similarly, the shear anisotropy [38] is:

$$A = \frac{2C_{44}}{C_{11} - C_{22}} = \frac{C_{44}}{C_{66}} \tag{10}$$

Table 3
Principle Young's moduli and Poisson's ratios for the tri-arc ReB_2 crystal.

$S_{11} = 0.00166247$	$E_{11} = 601.5$	$v_{12} = 0.2478$
$S_{33} = 0.00105979$	$E_{33} = 943.6$	$v_{13} = 0.1362$
		$v_{31} = 0.2137$

For the tri-arc crystal, A = 1.11, which is nearly isotropic, in agreement with the hardness measurements performed on ReB_2 crystals grown by the flux method [8].

Knowledge of the elastic moduli enables one to calculate the principle Poisson's ratios listed in Table 3 according to the formula [32]:

$$v_{ij} = \frac{-S_{ij}}{S_{ii}} \tag{11}$$

The highest value, 0.2478, is for v_{12}, indicating a relatively low resistance to bond-angle changes for changes in the bond length, most likely as a result of the high degree of delocalized metal bonding for the layered Re atoms within the a–b plane. Conversely, v_{13} exhibits the lowest Poisson's ratio of 0.1362, because of the strong covalent bonding between rhenium and boron atoms in the direction of the c-axis. A typical value for Poisson's ratio of covalent materials is 0.1, and for metallic materials 0.3, consistent with the directional bonding of ReB_2.

From the elastic moduli, the Debye temperature (θ_D) is computed for ReB_2. The Debye temperature correlates with many physical properties of solids that arise from atomic vibrations, such as melting point, thermal expansion and specific heat. Anderson [39] approximated θ_D from the −3 moment of the mean sound speeds, where:

$$v_t = \sqrt{\frac{G}{\rho}} \tag{12}$$

$$v_l = \sqrt{\frac{B + \frac{4}{3}G}{\rho}} \tag{13}$$

are the mean shear and compressional speeds, respectively, and:

$$v_m = \left[\frac{1}{3}\left(\frac{2}{v_t^3} + \frac{1}{v_l^3}\right)\right]^{1/3} \tag{14}$$

is the −3 moment. The Debye temperature can be calculated from the equation:

$$\theta_D = \frac{h}{k}\left[\frac{3n}{4\pi}\left(\frac{N_A\rho}{M}\right)\right]^{1/3} v_m \tag{15}$$

where h is Plank's constant, k is Boltzmann's constant, N_A is Avogadro's number, ρ is the density of the material, M is the molecular weight, and n is the number of atoms in the molecule (n = 3 for ReB_2). Substitution of the measured ambient-temperature elastic moduli and density (12.509 g cm^{-3}) of the tri-arc ReB_2 crystal yields a mean sound velocity of 5164 m s^{-1} and a Debye temperature of 734 K. Alternatively, when the single crystal elastic constants are known, v_m can be more accurately derived by averaging phase velocities in the sample over many directions [40]. For ReB_2, v_m was calculated using 4096 random vectors in one octant of the coordinate space, yielding a Debye temperature of 731 K, in good agreement with our initial calculation. This value does not correct for thermal

expansion and changes in moduli at the low temperatures where the Debye model is expected to be valid.

4. Conclusions

Resonant ultrasound spectroscopy was used on three different forms of superhard rhenium diboride, two isotropic polycrystals and one hexagonal-symmetry crystal, to measure the complete elastic modulus tensor. The measured moduli are strongly dependent on the morphology of the samples and the presence of excess boron. The elastic moduli for the ReB_2 crystal are remarkably high, with one modulus, $C_{33} = 1022$ GPa, nearly equal to that of diamond. The estimated mean shear modulus of 273 GPa and the observed bulk modulus agree well with previously reported experimental data. The Poisson's ratios support a model of strong covalent bonding along the *c*-axis and metallic bonding in the basal plane. A relatively high value of 731 K is reported for the (ambient temperature) Debye temperature of ReB_2.

Acknowledgements

This work is supported by the National Science Foundation grants DMR-0805357 (JBL, RBK), DMR-0654118 (JBB, AM), an IGERT Fellowship (JBL) and the State of Florida. The authors thank B.E. Weaver for collecting the nanoindentation data.

References

[1] Chung H-Y, Weinberger MB, Levine JB, Cumberland RW, Kavner A, Yang J-M, et al. Science 2007;318:1550d.
[2] Chung H-Y, Weinberger MB, Levine JB, Kavner A, Yang J-M, Tolbert SH, et al. Science 2007;316:436.
[3] Chung H-Y, Weinberger MB, Yang J-M, Tolbert SH, Kaner RB. Appl Phys Lett 2008;92:261904.
[4] Chung H-Y, Yang JM, Tolbert SH, Kaner RB. J Mater Res 2008;23:1797.
[5] Cumberland RW, Weinberger MB, Gilman JJ, Clark SM, Tolbert SH, Kaner RB. J Am Chem Soc 2005;127:7264.
[6] Gu Q, Krauss G, Steurer W. Adv Mater 2008;20:3620.
[7] Latini A, Rau JV, Ferro D, Teghil R, Albertini VR, Barinov SM. Chem Mater 2008;20:4507.
[8] Levine JB, Nguyen SL, Rasool HI, Wright JA, Brown SE, Kaner RB. J Am Chem Soc 2008;130:16953.
[9] Hao X, Xu Y, Wu Z, Zhou D, Liu X, Cao X, et al. J Phys Rev B 2006;74:224112/1.
[10] Hao X, Xu Y, Wu Z, Zhou D, Liu X, Meng J. J Alloy Compd 2008;453:413.
[11] Hao XF, Wu ZJ, Xu YH, Zhou DF, Liu XJ, Meng J. J Phys Condens Matter 2007;19:196212.
[12] Liang Y, Zhang B. Phys Rev B 2007;76:132101/1.
[13] Wang M, Li Y, Cui T, Ma Y, Zou G. Appl Phys Lett 2008;93:101905.
[14] Wang YX. Appl Phys Lett 2007;91:101904/1.
[15] Yang J, Sun H, Chen C. J Am Chem Soc 2008;130:7200.
[16] Zhang RF, Veprek S, Argon AS. Appl Phys Lett 2007;91:201914/1.
[17] Zhou W, Wu H, Yildirim T. Phys Rev B 2007;76:184113/1.
[18] Simunek A. Phys Rev B (Condens Matter Mater Phys) 2007;75:172108.
[19] Dubrovinskaia N, Dubrovinsky L, Solozhenko VL. Science 2007;318:1550c.
[20] Qin J, He D, Wang J, Fang L, Lei L, Li Y, et al. Adv Mater 2008;20:4780.
[21] La Placa S, Post B. Acta Crystallogr 1962;15:97.
[22] Oliver WC, Pharr GM. J Mater Res 1992;7:1564.
[23] Migliori A, Darling TW, Baiardo JP. In: Levy M, Bass H, Stern R, editors. Handbook of elastic properties of solids, liquids, and gases, vol. 1. New York: Academic Press; 2001. p. 239.
[24] Migliori A, Maynard JD. Rev Sci Instrum 2005:76.
[25] Migliori A, Sarrao J. Resonant ultrasound spectroscopy. New York: Wiley; 1997.
[26] Migliori A, Sarrao JL, Visscher WM, Bell TM, Lei M, Fisk Z, et al. Physica B 1993;183:1.
[27] Otani S, Aizawa T, Ishizawa Y. J Alloy Compd 1997;252:L19.
[28] Locci AM, Licheri R, Orru R, Cao G. Ceram Int 2009;35:397.
[29] Okada S, Kudou K, Lundstrom T. Jpn J Appl Phys Part 1 1995;34:226.
[30] Reuss A, Angew Z. Math Mech 1929;9:55.
[31] Voigt W. Lehrbuch der Kristallphysik. Leipzig: B.G. Teubner; 1910.
[32] Migliori A, Ledbetter H, Thoma DJ, Darling TW. J Appl Phys 2004;95:2436.
[33] Hill R. Proc Phys Soc Lond 1952;65:349.
[34] Solozhenko VL, Dub SN, Novikov NV. Diam Relat Mater 2001;10:2228.
[35] Tkachev SN, Solozhenko VL, Zinin PV, Manghnani MH, Ming LC. Phys Rev B 2003;68:052104.
[36] Koehler MR, Keppens V, Sales BC, Jin RY, Mandrus D. J Phys D – Appl Phys 2009;42:4.
[37] Migliori A, Ledbetter H, Leisure RG, Pantea C, Betts JB. J Appl Phys 2008;104:053512.
[38] Steinle-Neumann G, Stixrude L, Cohen RE. Phys Rev B 1999;60:791.
[39] Anderson OL. J Phys Chem Solid 1963;24:909.
[40] The codes used for the calculation are available from the National High Magnetic Field Laboratory. Resonant Ultrasound Spectroscopy Group. <http://www.magnet.fsu.edu/inhouseresearch/rus/index.html>.